Resonant Raman scattering by acceptors in GaAs/$Al_xGa_{1-x}As$ multiple quantum wells: A probe of exciton localization

I. Brener and E. Cohen
Solid State Institute and Physics Department, Technion–Israel Institute of Technology, Haifa 32000, Israel

Arza Ron
Solid State Institute and Chemistry Department, Technion–Israel Institute of Technology, Haifa 32000, Israel

L. Pfeiffer
AT&T Bell Laboratories, Murray Hill, New Jersey 07974

(Received 1 June 1990; revised manuscript received 30 July 1990)

We report a study of the electronic Raman scattering (ERS) by residual acceptors and of LO-phonon resonant Raman scattering in undoped multiquantum wells (MQW's). The samples studied are GaAs/$Al_xGa_{1-x}As$ MQW's with $x=0.3$ and 1 and well widths $L=40$ and 70 Å. The spectral range under study is the vicinity of the $(e_1{:}hh_1)1S$ exciton band (where hh denotes heavy hole) and the experiments were carried out at low temperatures ($T=2$ K). The scattering transition involved in the ERS is the hole transition $1S_{3/2}(\Gamma_6\rightarrow\Gamma_7)$. The ERS shows a superlinear dependence on the exciting laser power. This is due to the creation of neutral acceptors by the exciting laser beam, which increases the concentration of scattering centers. For a laser intensity of ~ 300 W/cm^2, we find that the ERS cross section is at least eight orders of magnitude larger than the LO-phonon Raman-scattering cross section. The ERS resonates at energies in the low-energy tail of the intrinsic $(e_1{:}hh_1)1S$ exciton band. We identify this spectral range as the acceptor–bound-exciton band (A^0,X). On the other hand, the LO-phonon Raman scattering resonates at an energy corresponding to the delocalized intrinsic $(e_1{:}hh_1)1S$ exciton band as measured in photoluminescence excitation experiments. The ERS resonance profile has an asymmetric shape with a cutoff on its high-energy side. We show that this sharp decrease in the scattering cross section is due to an increase of the (A^0,X) damping factor Γ, which reflects the tunneling between (A^0,X) and intrinsic $(e_1{:}hh_1)1S$ exciton states. We present a model that accounts for the measured ERS resonance profile in which the (A^0,X) damping factor is assumed to be proportional to the $(e_1{:}hh_1)1S$ exciton density of states.

I. INTRODUCTION

The luminescence in direct-gap semiconductors at low temperatures is dominated by bound-exciton recombination. Particularly, in bulk GaAs of good quality, neutral donor and acceptor bound excitons, (D^0,X) and (A^0,X), give rise to emission lines that are well resolved from the free $1S$ exciton band. The situation in GaAs/$Al_xGa_{1-x}As$ quantum wells (QW's) is more complex, as excitons can also be localized by potential fluctuations due to interface roughness, with binding energies of the same order of magnitude as those of (A^0,X) or (D^0,X). These intrinsic excitons are in the $(e_1{:}hh_1)1S$ state (where hh denotes heavy hole), and the corresponding spectral band is inhomogeneously broadened. Photoluminescence studies, both cw (Ref. 1) and time resolved,[2] were done under selective excitation within the $(e_1{:}hh_1)1S$ band. Hole burning,[3] transient grating,[4] and photon-echo spectroscopy[5] were also studied. All these experiments lead to the description of excitons localized on interface roughness in the low-energy tail of the $1S$ band and extended excitons in the upper part of this band. Light-scattering experiments involving LO phonons are usually reported for excitation in the spectral range of $(e_2\text{-}hh_2)$ or higher electronic transitions.[6] However, under resonant excitation of the $(e_1{:}hh_1)1S$ exciton band, LO-phonon Raman scattering can also be used in order to study exciton localization.[7,8]

Recently, the electronic Raman scattering (ERS) by residual acceptors in undoped QW's has been used in order to probe the nature of the $(e_1{:}hh_1)$ excitons at low temperatures.[9] This scattering process is resonantly enhanced when impurity bound excitons act as intermediate states. Similarly, ERS by intersubband transitions in doped QW's has been shown to be resonantly enhanced when free excitons act as intermediate states.[10] In ERS experiments involving impurities, the bound electron (or hole) is promoted to a higher electronic level of the neutral donor (D^0) or acceptor (A^0). These levels can be any of the higher nL multiplets. The confining well potential splits the degenerate hole energy levels of the acceptor. Particularly, the ground $1S_{3/2}$ level is split into two Kramers doublets (Γ_6,Γ_7).[11] Their separation Δ has been calculated by Masselink, Chang, and Morkoç[12] and was found to be in the range of $\sim 2-10$ meV, depending on the well width L, and on the acceptor location in the well. ERS has been observed[13,14] between these Γ_6 and Γ_7 levels in doped GaAs/$Al_xGa_{1-x}As$ mul-

tiquantum wells (MQW's) with $L \lesssim 100$ Å. The calculated values of Δ agree with the observed ones, both for acceptor doping at the center and at the edge of the well.

In an undoped QW there are always background impurities. The compensated donors and acceptors are all ionized at low temperatures. In order to observe ERS involving internal transitions, the ionized impurities must be neutralized. This is achieved by the exciting laser beam. The distribution of acceptor impurity locations in an undoped QW is unknown. However, the acceptor location will affect both the A^0 binding energies and the splitting of its ground state. In principle, the binding energies of neutral acceptor bound excitons, (A^0,X), are also dependent on the location in the well. However, since the binding energy is essentially independent of the acceptor species in bulk GaAs,[15] it is expected that the binding energies will be mainly determined by the potential fluctuation in the near vicinity of the A^0 atom. Therefore, the (A^0,X) band will be inhomogeneously broadened and will overlap the tail of the localized intrinsic exciton band.[16] In this overlap spectral region, tunneling between localized states in expected. The consequences of this tunneling on the ERS involving neutral acceptors are the main subject of this paper.

We report on a study of the ERS by acceptors in undoped GaAs/AlAs ($L = 70$ Å) and GaAs/$Al_{0.28}Ga_{0.72}As$ ($L = 40$ Å) MQW's. The scattering transition involved is $1S_{3/2}(\Gamma_6 \rightarrow \Gamma_7)$, and its intensity was measured as a function of the laser energy (E_L). In this way, the ERS profile, $\sigma_{A^0}(E_L)$, was obtained in the spectral range of the inhomogeneously broadened $(e_1{:}hh_1)1S$ exciton band. It is shown that this ERS resonates strongly in the energy region which corresponds to localized excitons. Furthermore, since the scattering process involves internal acceptor transitions, we identify these localized excitons as (A^0,X). The resonant Raman scattering (RRS) by LO phonons was also studied in the same spectral region. Its profile $\sigma_{LO}(E_L)$ is compared with $\sigma_{A^0}(E_L)$ and it is found that $\sigma_{LO}(E_L)$ resonates at the energy which corresponds to the maximum density of states of the intrinsic excitons. The sharp cutoff of the measured $\sigma_{A^0}(E_L)$ provides a new way of probing exciton levels with different dynamical properties. Thus, we show that the ERS complements the methods of spectral hole burning[3] and transient grating spectroscopy[4] in analyzing exciton localization in MQW's.

The paper is laid out as follows. Section II gives the experimental details. In Sec. III we analyze the ERS and compare its resonance profile and intensity with those of the LO-phonon RRS. Section IV summarizes this study.

II. EXPERIMENT

Two undoped, samples grown by molecular beam epitaxy were studied: the first one consists of 50 wells of GaAs of thickness 70 Å separated by 200-Å layers of AlAs (sample 1). The second one has ten 40-Å layers of GaAs separated by 200-Å layers of $Al_{0.28}Ga_{0.72}As$ (sample 2). The buffer layer of both samples is GaAs which was grown under the same conditions as the MQW's.

The experiments were performed with the samples immersed in liquid He. Excitation was done using a cw dye laser with Pyridine 2 dye. The laser linewidth was less than 0.2 meV. The detection was performed using a double spectrometer and standard photon-counting equipment.

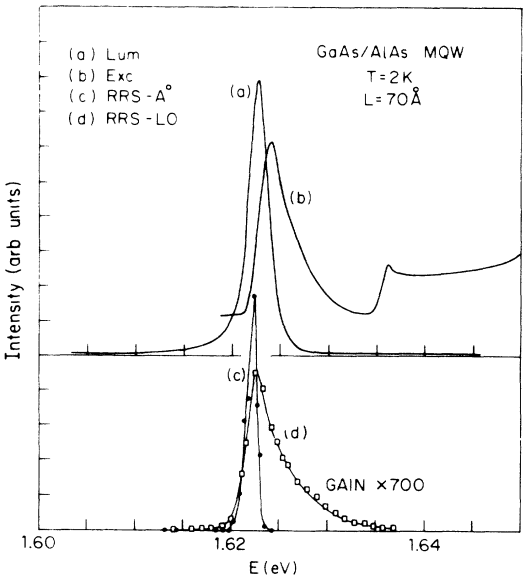

FIG. 1. (a) Luminescence and (b) its excitation spectra for sample 1. The latter was monitored at 1.623 eV. (c) The intensity of the A_3 line of the neutral acceptor electronic Raman scattering and (d) of the LO-phonon scattering as a function of incident laser energy. The laser intensity was 100 W/cm^2. The solid lines in (c) and (d) serve as a guide to the eye.

Figure 1(a) shows the photoluminescence spectrum of sample 1, and Fig. 1(b) shows its excitation spectrum monitored at 1.623 eV. Figures 2(a) and 2(b) show the

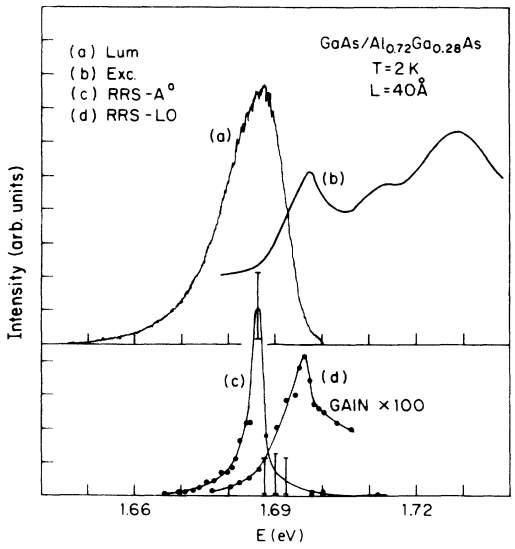

FIG. 2. Same as Fig. 1 but for sample 2. The photoluminescence excitation spectrum was monitored at 1.661 eV.

corresponding spectra of sample 2. The ERS is only observed when the excitation is into the low-energy tail of the exciton band. Typical spectra are shown in Fig. 3 for the two samples under study and for a laser intensity of ~ 100 W/cm^2 (A_i denote the ERS lines). For weaker laser intensities, a multitude of ERS lines can be resolved. As the laser intensity is increased, the number of lines decreases and, finally, one broad ERS line dominates the Raman spectrum. This is depicted in Fig. 4, where ERS spectra are shown for different laser intensities. For the weakest laser intensities used ($\lesssim 10^{-1}$ W/cm^2) only the LO-phonon Raman lines could be resolved, whereas for the highest intensities used (~ 300 W/cm^2) the ERS lines were about 1000 times more intense than the LO-phonon RRS. Figure 5 shows the intensity dependence of the ERS and LO-phonon Raman lines.

The Raman spectra were recorded in the $z(xx)\bar{z}$, $z(xy)\bar{z}$, $z(x'x')\bar{z}$, and $z(x'y')\bar{z}$ configurations, where $x=[100]$, $y=[010]$, $x'=[110]$, $y'=[1\bar{1}0]$ and z is the growth axis [001]. Unlike the LO-phonon Raman scattering which is $z(xx)\bar{z}$ polarized, the ERS lines were found to be unpolarized. Figures 1(c), 1(d), 2(c), and 2(d) show the ERS and LO-phonon Raman-scattering intensities as a function of the incident laser energy for the two samples under study: the Raman resonance profiles. The line A_3 was used to draw the ERS profiles shown in these figures (as well as the intensity dependence in Fig. 5). The resonant Raman profiles are not corrected for absorption. The reason for that is as follows: the total widths of the GaAs wells are 3500 and 400 Å for samples 1 and 2, respectively. At the peak of the exciton band, the absorption coefficient is[17] $\sim 4\times 10^4$ cm^{-1}. Thus the light intensity is reduced by a factor of 3 at the most, over the whole MQW. Moreover, the ERS resonates well below the absorption peak. Therefore, this absorption correction is negligible in comparison to the abrupt drop (by a factor of $\sim 10^3$) in the high-energy part of the ERS profile.

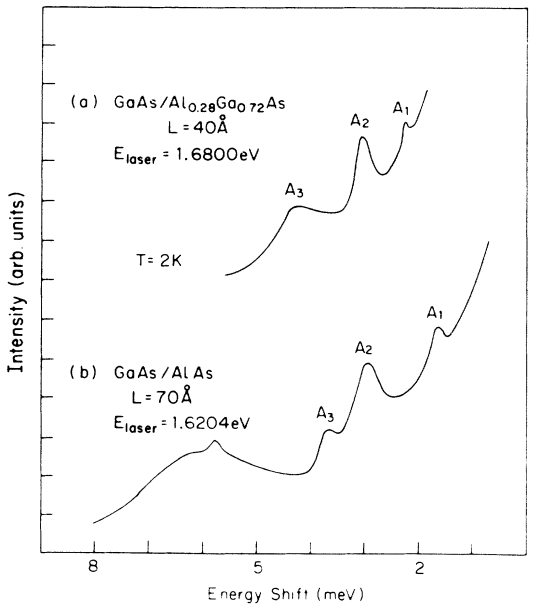

FIG. 3. Typical neutral acceptor ERS spectra observed in both samples upon excitation into the lower part of the $(e_1{:}hh_1)1S$ exciton band. The laser intensity used was 100 W/cm^2.

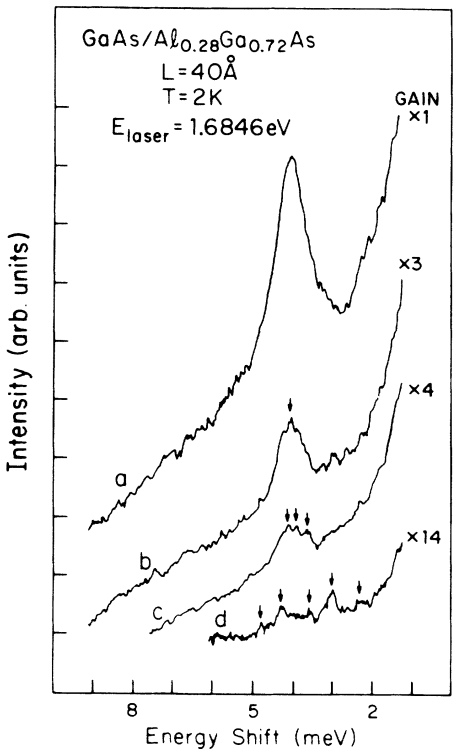

FIG. 4. ERS spectra recorded at different exciting laser intensities: (a) $I_{in}=150$ W/cm^2. (b) $I_{in}=21$ W/cm^2, (c) $I_{in}=12$ W/cm^2, (d) $I_{in}=6$ W/cm^2. The arrows indicate ERS lines.

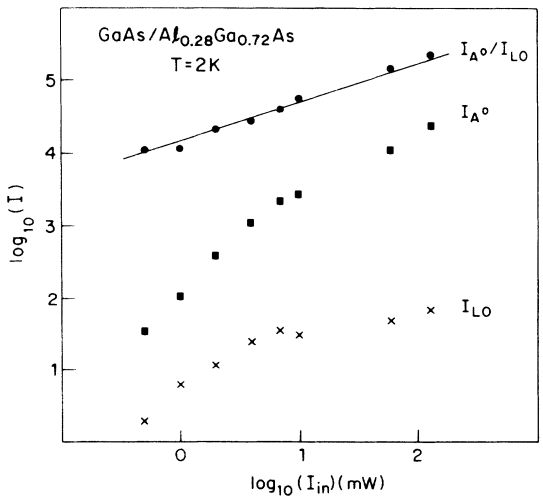

FIG. 5. Laser power dependence of the ERS intensity I_{A^0} (line A_3 of Fig. 3) and of the LO-phonon Raman-scattering intensity I_{LO}. The top curve is fitted to $I_{in}^{0.5}$.

III. ANALYSIS

A. Identification of the ERS lines

We first consider the origin of the A_i lines. Gammon *et al.*[13] have observed ERS lines due to the different acceptor transitions in Be-doped GaAs/$Al_xGa_{1-x}As$ MQW's. Besides the ERS lines corresponding to the $1S_{3/2} \rightarrow 2S_{3/2}$ hole transitions, they observed a single ERS line corresponding to the $1S_{3/2}(\Gamma_6 \rightarrow \Gamma_7)$ transition (denoted "*C* line" in their papers). Its energy, Δ, depended on whether the MQW structure was doped at the well center or close to the interface and agreed with the theoretical predictions[12] of $\Delta \sim 2-10$ meV. Our experiments were carried out on undoped MQW's. The series of lines denoted A_i in Fig. 3, which are obtained upon resonant excitation into the $(e_1{:}hh_1)$ exciton band, are assigned to ERS by the following considerations.

(a) Their energy separation from the laser line is constant (the energy spacings are in the range of the calculated Δ).

(b) The A_i lines are sharp (width of about 0.5 meV).

(c) Under intense excitation, the anti-Stokes line of A_3 is observed.

The multiplet of ERS lines observed at low laser intensities is attributed by us to scattering by acceptors in distinct locations in the quantum well (and thus they have a different ground-state splitting). The small number of ERS lines, which dominate the Raman spectrum under high-intensity excitation, reflects the most abundant A^0 sites in the QW. Although intuitively one would have expected a uniform distribution of background acceptors, the distinct ERS lines indicate that there are preferred sites in the QW. We did not observe ERS lines due to the hole transition $1S_{3/2} \rightarrow 2S_{3/2}$, although previous studies of this kind of ERS report observing these transitions.[13,14,18]

The ERS intensity shows a superlinear dependence on the laser intensity. This is shown in Fig. 5. We find it useful to compare I_{A^0} with that of the LO-phonon scattering (for the same excitation energy): $I_{A^0}/I_{\rm LO} \propto I_{\rm in}^{0.5\pm0.1}$. $I_{\rm LO}$ by itself shows a sublinear dependence. This cannot be due to heating of the sample by the laser light, since the absorption coefficient at these excitation energies is relatively small ($\alpha \lesssim 10^3$ cm^{-1}). Both the ERS and the LO-phonon RRS intensities depend on dynamical processes which affect the exciton damping (see below). The fact that the ERS has a stronger dependence on $I_{\rm in}$ than that of the LO-phonon RRS is interpreted as increasing the concentration of A^0 due to acceptor neutralization by the exciting laser beam.[19]

We can estimate the density of A^0 by examining the emission spectrum of the buffer layer, which is grown under the same conditions as the MQW. Therefore, background impurities which are incorporated during the growth process are expected to have the same concentration in both the buffer layer and the MQW. The GaAs buffer layer shows weak (e-A^0) and (D^0-A^0) bands whose intensities relative to the free exciton line are typical[20] of crystals with $n(A^0) < 10^{15}$ cm^{-3}. This means that the areal density of A^0 in the MQW is less than 10^9 cm^{-2}.

B. The ERS profile

For simplicity sake let us first consider the ERS cross section for the case of a single neutral acceptor species. Its split ground-state levels are $|A^0,\Gamma_6\rangle$ and $|A^0,\Gamma_7\rangle$ with $\Delta = E(\Gamma_7) - E(\Gamma_6)$. The exciton bound to this acceptor has eigenstates $|n\rangle = |(A^0,X),nS\rangle$ with energies E_n. Although in principle we should sum over all the possible intermediate states in the Raman-scattering matrix element, only nS states will contribute significantly to the resonant ERS (in fact, we shall consider below only the $1S$ state). The scattering matrix element is given by[21,22]

$$\tilde{K}^{A^0}_{\alpha\beta}(E_L) = \sum_n \left[\frac{\langle A^0,\Gamma_7|p_\beta|n\rangle\langle n|p_\alpha|A^0,\Gamma_6\rangle}{E_n - E_L + i\Gamma(E_n)} + \frac{\langle A^0,\Gamma_7|p_\beta|n\rangle\langle n|p_\alpha|A^0,\Gamma_6\rangle}{E_n + (E_L+\Delta) + i\Gamma(E_n)} \right], \tag{1}$$

where E_L is the laser energy, $\Gamma(E_n)$ is the phenomenological exciton damping factor, and $\mathbf{p}$ denotes the electric dipole operator. The ERS cross section is taken as

$$\sigma_{A^0}(E_L) = C_A[\mathrm{Im}(\hat{\mathbf{e}}_S \tilde{K}^{A^0} \hat{\mathbf{e}}_L)]^2 . \tag{2}$$

$\hat{\mathbf{e}}_L$ and $\hat{\mathbf{e}}_S$ are the incident and scattered beam polarization vectors, respectively, and C_A lumps up all the pertinent constants. A strong resonance is observed only in the spectral range of $E_L \sim E((A^0,X)1S) \equiv E$. As will be shown below, the exciton damping increases sharply with increasing exciton energy. Therefore, only the first term in Eq. (1) will contribute significantly to the cross section.

We now consider the effects of the QW interface roughness. They give rise to potential fluctuations to which both the A^0 and the (A^0,X) are subjected. The distribution of interface roughness leads to an inhomogeneously broadened $(A^0,X)1S$ band which we describe by a density of states $\rho_{(A^0,X)}(E)$. For a random distribution of potential fluctuations, $\rho_{(A^0,X)}(E)$ is expected to be a Gaussian. The $(A^0,X)1S$ band overlaps the low-energy tail of the band due to excitons localized by interface potential fluctuations. Thus, tunneling from the (A^0,X) states will determine the acceptor–bound-exciton damping, $\Gamma(E)$. $\rho_{(A^0,X)}(E)$ can then be subdivided into densities of states according to the exciton damping factor[23] $\rho_{(A^0,X)}(E,\Gamma)$ and

$$\rho_{(A^0,X)}(E) = \int_{\Gamma_m(E)}^{\infty} \rho_{(A^0,X)}(E,\Gamma)\,d\Gamma . \tag{3}$$

Γ_m is the minimum damping factor of the (A^0,X) excitons which have an energy between E and $E+dE$. The ERS cross section is then given by

$$\sigma_{A^0}(E_L)=C_A\int dE\int d\Gamma\frac{|\langle A^0,\Gamma_7|p_\beta|(A^0,X)1S\rangle\langle(A^0,X)1S|p_\alpha|A^0,\Gamma_6\rangle|^2}{(E-E_L)^2+\Gamma^2(E)}\Gamma(E)\rho_{(A^0,X)}(E,\Gamma(E)) . \quad (4)$$

For a given energy E, it is sufficient to consider the (A^0,X) states with the lowest damping factor, $\Gamma_m(E)$. Then Eq. (4) can be simplified to

$$\sigma_{A^0}(E_L)=C'_A\int dE\frac{\Gamma_m(E)\rho_{(A^0,X)}(E)}{(E-E_L)^2+\Gamma_m^2(E)} . \quad (5)$$

In the last step, we have assumed that the transition dipole matrix elements are independent of energy.

If the damping processes were slow and independent of (A^0,X) sites, then $\sigma_{A^0}(E_L)$ will be proportional to $\rho_{(A^0,X)}(E_L)$.[23] In that case, assuming an inhomogeneously broadened (A^0,X) band, $\sigma_{A^0}(E_L)$ is expected to be a Gaussian. As can be seen in Figs. 1(c) and 2(c), this is clearly not the case. The abrupt high-energy cutoff observed for $\sigma_{A^0}(E_L)$ is interpreted as a result of a large increase in $\Gamma_m(E)$. This increase must be due to fast tunneling between (A^0,X) states and intrinsic exciton states which coexist at the energy of the $\sigma_{A^0}(E_L)$ cutoff. This is schematically depicted in Fig. 6.

We do not have *a priori* information on the dependence of the exciton damping on its energy. Therefore, as a first approximation we assume that $\Gamma_m(E)$ is proportional to the density of intrinsic localized excitons (ρ_{FE}) to which the (A^0,X) excitons can tunnel. This will be taken as the intrinsic exciton density of states at the same energy E as that of the excited (A^0,X). Since for energies below the $(e_1{:}hh_1)1S$ delocalized exciton level this density of states can be well described by an exponential tail, we will take

$$\Gamma_m(E)=\exp\left[-\left[\frac{E-E_\Gamma}{\Delta E_\Gamma}\right]\right] , \quad (6)$$

where E_Γ and ΔE_Γ are parameters to be determined by a fit to the observed Raman profile. Figures 7(b) and 7(c) show the fits obtained with Eqs. (5) and (6) and a Gaussian (A^0,X) density of states,

$$\rho_{(A^0,X)}(E)\propto\exp\{-[(E-E_{(A^0,X)})/\Delta E_{(A^0,X)}]^2\} .$$

Figure 7(a) shows the functions $\Gamma_m(E)$ and $\rho_{(A^0,X)}(E)$ for sample 1. Table I lists the parameters used for the calculations.

From $E_{(A^0,X)}$ and the knowledge of the $(e_1{:}hh_1)1S$ exciton energy level [as measured from photoluminescence excitation (PLE)], we can obtain the (A^0,X) binding energies for the two samples under study. They are 2.5 meV for the 70-Å sample and 8.5 meV for the 40-Å one. GaAs/Al_xGa_{1-x}As QW's which are heavily doped with Be at the center of the wells[24] exhibit an (A^0,X) luminescence peak which is well separated from the intrinsic exciton band. In our experiments, on the other hand, the peak of $\rho_{(A^0,X)}(E)$ obtained by fitting the experimental

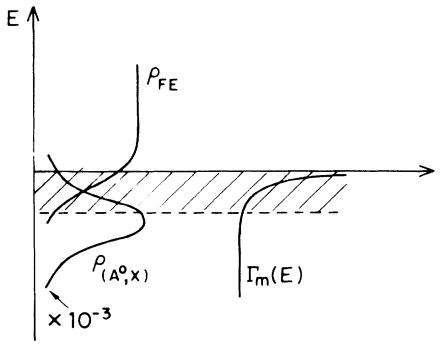

FIG. 6. A schematic description of the intrinsic $(e_1{:}hh_1)1S$ exciton density of states ρ_{FE} and the (A^0,X) density of states $\rho_{(A^0,X)}$. The damping factor of the (A^0,X) states increases with increasing tunneling rate to the intrinsic exciton states available at the same energy.

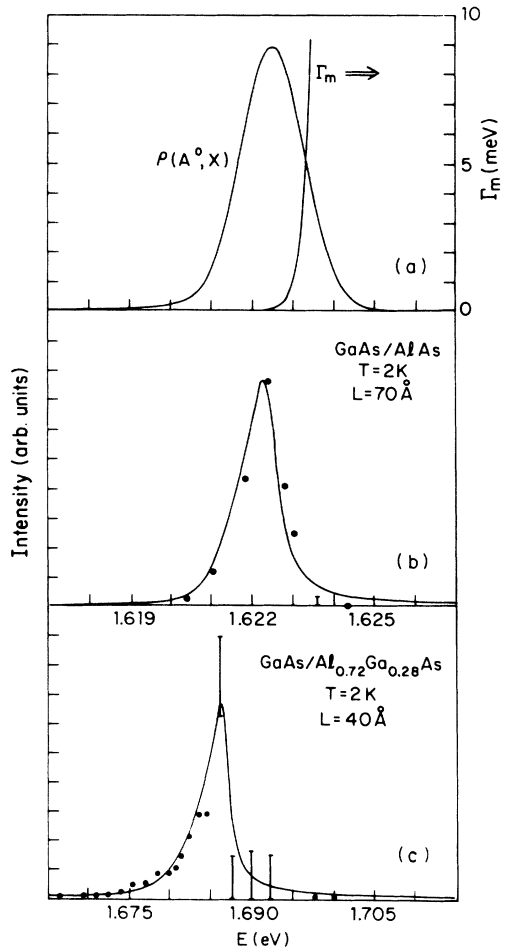

FIG. 7. (a) The (A^0,X) damping factor $\Gamma_m(E)$ and density of states $\rho_{(A^0,X)}$ for sample 1 used in the calculations. (b) and (c) show the model fit to the experimental ERS profile for samples 1 and 2, respectively.

TABLE I. Parameters used for the calculations. E_{FE} denotes the energy of the $(e_1{:}hh_1)1S$ exciton as measured by PLE.

Parameter	Sample 1 (70 Å)	Sample 2 (40 Å)
E_Γ	1.6230 eV	1.6929 eV
Δ_Γ	0.2 meV	0.5 meV
E_{FE}	1.6250 eV	1.6959 eV
$E_{(A^0,X)}$	1.6225 eV	1.6874 eV
$\Delta E_{(A^0,X)}$	1.1 meV	7.8 meV

ERS profile overlaps the luminescence band. A possible explanation to the difference between these observations is that the acceptors responsible for the ERS in undoped samples accumulate near the interface thus allowing a lower (A^0,X) binding energy. Moreover, tunneling between (A^0,X) states will be efficient in highly doped QW's. Therefore the luminescence of such QW's will always be due to the lower tail of the (A^0,X) band. This will result in a large splitting between the (A^0,X) luminescence and that due to intrinsic, localized excitons as reported in Ref. 24.

C. Comparison with the LO-phonon RRS

The LO-phonon Raman scattering cross section is given by third-order perturbation theory. The Raman-scattering matrix element is[21]

$$\tilde{K}_{\alpha\beta}^{\mathrm{LO}}=\sum_{n,m}\frac{\langle f|p_\beta|m\rangle\langle m|H_{EL}|n\rangle\langle n|p_\alpha|i\rangle}{(E_n-E_L+i\Gamma_n)(E_m-E_L+i\Gamma_m)} \quad . \tag{7}$$

Here H_{EL} is the exciton-phonon interaction Hamiltonian and the summation has to be carried over all the intermediate exciton states $|n\rangle$ and $|m\rangle$. There are five other nonresonant terms which we have excluded from Eq. (7). Two resonances are usually observed in the LO-phonon Raman profile: the incoming and outgoing beam resonances, which correspond to the vanishing of the denominator in the last equation. The resonance in σ_{LO}, shown in Figs. 1(d) and 2(d), corresponds to the incoming beam resonance (the outgoing beam resonance is obtained at a higher energy and is not shown in these figures). It should be noted that the modifications in $\tilde{K}^{\mathrm{LO}}$, which give rise to the "forbidden" RRS shown here, can be incorporated in the expression for $\langle m|H_{EL}|n\rangle$, as is the case for the Fröhlich interaction.[22]

The LO-phonon Raman-scattering profile, $\sigma_{\mathrm{LO}}(E_L)$, peaks in the spectral region of efficient excitation of the luminescence [Figs. 1, 2(b), and 2(d)].[7] The emission is weak in this region and this spectral range was identified as being part of the delocalized excitons. Moreover, from the ratio of the outgoing to the incoming beam resonances,[7] these delocalized excitons have been shown to be strongly scattered by the imperfections in the well. Their large density of states is a major contributor to the resonance LO-phonon Raman enhancement.

We can compare the intensities of the two Raman-scattering processes, namely electronic versus LO-phonon Raman scattering for the same E_L. For laser intensities greater than 100 W/cm^2, the measured intensity of the former is found to be three orders of magnitude stronger than the latter. Two factors contribute to this large disparity. First, the LO-phonon RRS is a third-order scattering process, whereas the ERS is a second-order process, as can be seen by comparing Eqs. (1) and (7). Second, the measured Raman scattering is proportional to $\sigma\rho_f$, where σ is the scattering cross section and ρ_f is the final density of states of the system. For the highest laser intensities used, we can assume that the acceptors are fully neutralized. Hence, we use the estimated density of acceptors given in Sec. III A, so that $\rho_{f,A^0}\sim 10^{14}$ cm^{-3}. As regarding the LO-phonon Raman scattering, the final density of states is given by the density of LO phonons for the k vector involved in the scattering process. From previous studies,[7] it is known that the k-vector conservation rule in one LO Raman scattering in MQW's is relaxed as a consequence of a finite spread in k space of the $(e_1{:}hh_1)1S$ exciton states. For order-of-magnitude estimates, we can take this spread as $\Delta k\sim 10^{-3}k_{\mathrm{BZ}}$, where k_{BZ} is the Brillouin-zone k vector. Therefore, $\rho_{f,\mathrm{LO}}\sim 10^{19}$ cm^{-3}. Since tunneling between (A^0,X) and intrinsic excitons is important at the spectral range we are considering we can assume that their damping factors are of the same order of magnitude. Therefore the scattering cross-sections ratio will be

$$\frac{\sigma_{A^0}}{\sigma_{\mathrm{LO}}}\sim 10^8 \quad . \tag{8}$$

It should be noted that very large enhancements of the ERS cross section have been observed in bulk CdTe and GaAs.[25,26]

IV. SUMMARY

We presented a study of the ERS by residual acceptors in undoped MQW's and compared it to the LO-phonon RRS. We showed that the former sharply resonates in the low-energy tail of the excitonic emission. We have identified this resonance with the (A^0,X) band, which spans the same energy range as the intrinsic $(e_1{:}hh_1)1S$ excitons localized by interface potential fluctuations. On the other hand, the LO-phonon Raman-scattering resonates in the spectral range of the delocalized intrinsic excitons band. The superlinear intensity dependence on exciting laser power of the ERS is attributed to the neutralization of acceptors by the laser light. This increases the density of A^0 scattering centers. For a laser intensity of ~ 300 W/cm^2 it was found that the ERS cross section is at least eight orders of magnitude larger than the LO-phonon Raman-scattering cross section.

The ERS resonance profile has a sharp cutoff on its high-energy side. We showed that this is directly related to an energy-dependent damping factor Γ_m of the (A^0,X) states. We analyzed the ERS cross section by means of a model which assumes a Γ_m proportional to the tunneling rate between (A^0,X) states and intrinsic excitons. Hence, electronic Raman scattering by residual impurities proves to be an efficient method to study the dynamical proper-

ties of excitons in QW's and complementary to the experiments which can be carried in the time domain.

ACKNOWLEDGMENTS

The work done at the Technion was supported by the U.S.–Israel Binational Science Foundation, Jerusalem, and by the Fund for the Promotion of Research at the Technion. One of us (E.C.) acknowledges the support of the R. and M. Rochlin Research Fund. Another (A.R.) acknowledges the support of the P. and E. Nathan Research Fund.

[1]For a review, see for example G. Bastard, *Wave Mechanics Applied to Semiconductor Heterostructures,* Les èditions de physique, Paris, 1988.

[2]Y. Masumoto, S. Shionoya, and H. Kawaguchi, Phys. Rev. B **29**, 2324 (1984).

[3]J. Hegarty, Phys. Rev. B **25**, 4324 (1982).

[4]J. Hegarty, M. D. Sturge, A. C. Gossard, and W. Wiegmann, Appl. Phys. Lett. **40**, 132 (1982).

[5]L. Schultheis, M. D. Sturge, and J. Hegarty, Appl. Phys. Lett. **47**, 995 (1985).

[6]W. Kauschke, A. K. Sood, M. Cardona, and K. Ploog, Phys. Rev. B **36**, 1612 (1987).

[7]I. Brener, A. Ron, E. Cohen, and L. Pfeiffer, Superlatt. Microstruct. **5**, 223 (1989).

[8]J. E. Zucker, A. Pinczuk, D. S. Chemla, and A. C. Gossard, Phys. Rev. B **35**, 2892 (1987).

[9]I. Brener, E. Cohen, A. Ron, and L. Pfeiffer, Surf. Sci. (to be published).

[10]G. Danan, A. Pinczuk, J. P. Valladares, L. N. Pfeiffer, K. W. West, and C. W. Tu, Phys. Rev. B **39**, 5512 (1989).

[11]Y. C. Chang, Physica B+C **146B**, 137 (1987).

[12]T. Masselink, Y. C. Chang, and H. Morkoç, Phys. Rev. B **32**, 5190 (1985).

[13]D. Gammon, R. Merlin, W. T. Masselink, and H. Morkoç, Phys. Rev. B **33**, 2919 (1986).

[14]P. O. Holtz, M. Sundaram, R. Simes, J. L. Merz, A. C. Gossard, and J. H. English, Phys. Rev. B **39**, 13 293 (1989).

[15]D. J. Ashen, P. J. Dean, D. T. J. Hurle, J. B. Mullin, A. M. White, and P. D. Greene, J. Phys. Chem. Solids **36**, 1041 (1975).

[16]The term intrinsic is used to describe both excitons in extended states and those localized by potential fluctuations resulting from interface roughness.

[17]Y. Masumoto, M. Matsuura, S. Tarucha, and H. Okamoto, Phys. Rev. B **32**, 4275 (1985).

[18]K. T. Tsen, J. Klem, and H. Morkoç, Solid State Commun. **59**, 537 (1986).

[19]In bulk GaAs a saturation of this ERS was observed. See R. Bray, K. Wan, and J. C. Parker, Phys. Rev. Lett. **57**, 2434 (1986).

[20]E. S. Koteles, J. P. Salerno, W. Bloss, and E. M. Brody, *Proceedings of the 17th International Conference on the Physics of Semiconductors* (Springer-Verlag, Berlin, 1984), p. 1247.

[21]A. Pinczuk and E. Burstein, in *Light Scattering in Solids I,* edited by M. Cardona and G. Güntherodt (Springer-Verlag, Berlin, 1975), Chap. 2.

[22]M. Cardona, in *Light Scattering in Solids II,* edited by M. Cardona and G. Güntherodt (Springer-Verlag, Berlin, 1975), Chap. 2.

[23]D. Gershoni, E. Cohen, Arza Ron, and M. D Sturge, J. Lumin. **38**, 230 (1987).

[24]P. O. Holtz, M. Sundaram, J. L. Merz, and A. C. Gossard, Phys. Rev. B **40**, 10 021 (1989).

[25]R. G. Ulbrich, N. Van Hieu, and C. Weisbuch, Phys. Rev. Lett. **46**, 53 (1981).

[26]P. Y. Yu and L. M. Falicov, Phys. Rev. B **24**, 1144 (1981).